seem to exist in most compounds, one type being the major rotamer in the 4-H compounds **1**, **5**, **10**, and **12** but the minor rotamer in the four-substituted analogues. This type of double minima within one main conformer has often been inferred from molecular mechanics calculations,[40] but this is the first experimental proof for their existence. The MM2 force field is unexpectedly unsuccessful in predicting conformational energies, but the calculated minimum energy geometries are believed to be more reliable.

Acknowledgment. We thank the Swedish Natural Science Research Council, the French Centre National de la Recherche Scientifique, and the Knut and Alice Wallenberg Foundation for generous financial support. We also thank Dr. T. Liljefors for helpful advice with the molecular mechanics calculations, J. Glans for skillful recording of the CD spectra, Dr. I. Nilsson and Professors J. A. Schellman and G. Pfister-Guillouzo for making their computer programs available to us and for much good advice, and Professor T. D. Bouman and Dr. A. E. Hansen for providing us with data prior to publication.

Registry No. **1**, 96393-05-4; **2**, 96393-06-5; **3**, 105615-74-5; **4**, 105615-75-6; **5**, 105519-59-3; **6**, 105615-76-7; **7**, 105615-77-8; **8**, 105615-78-9; **9**, 105519-60-6; **10**, 105615-79-0; **11**, 105519-61-7; (±)-**12**, 96349-15-4; (±)-**13**, 96349-16-5; (±)-**14**, 96349-17-6; **15**, 17294-24-5; (*R*)-*N*-(1-phenylethyl)ammonium (*R*)-*N*-(1-phenylethyl)dithiocarbamate, 105660-54-6; (*R*,*S*)-1-amino-1,2,3,4-tetrahydronaphthalene, 32908-38-6; triethylammonium (*R*,*S*)-*N*-(1,2,3,4-tetrahydro-1-naphthyl)dithiocarbamate, 105519-63-9; chloroethanal, 107-20-0; 1-phenyl-2-bromoethanone, 70-11-1; 2-bromo-4-methyl-3-pentanone, 29583-93-5; 2-bromo-2-phenylethanal, 16927-13-2; 1-phenyl-2-bromo-1-propanone, 2114-00-3; (*S*)-*N*-(1-phenylethyl)ammonium (*S*)-*N*-(1-phenethyl)dithiocarbamate, 105519-65-1; CS_2, 75-15-0; (*R*)-1-phenylethylamine, 3886-69-9; chloropropanone, 78-95-5; 3-chloro-2-butanone, 4091-39-8; 1-bromo-3-methyl-2-butanone, 19967-55-6; 2-bromo-3-pentanone, 815-52-1; 1-bromo-1-phenyl-2-propanone, 23022-83-5; 2-bromopropanal, 19967-57-8.

Photooxidation of Tetraanionic Sensitizer Ions by Dihexadecyl Phosphate Vesicle-Bound Viologens

James K. Hurst,*† David H. P. Thompson,† and John S. Connolly‡

Contribution from the Department of Chemical and Biological Sciences, Oregon Graduate Center, Beaverton, Oregon 97006-1999, and Photoconversion Research Branch, Solar Energy Research Institute, Golden, Colorado 80401. *Received July 2, 1986*

Abstract: Triplet state lifetimes of several photoredox-active anions were shortened by adding *N*-alkyl-*N*-methyl-4,4′-bipyridinium (C_nMV^{2+}) ions in the presence of dihexadecyl phosphate (DHP) vesicles. Optical spectroscopic measurements indicate that the predominant reaction mechanism is one-electron oxidative quenching. For [5,10,15,20-tetrakis(4-sulfonatophenyl)porphinato]zinc(II) ($ZnTPPS^{4-}$) ion, yields of charge-separated product ions are high, so that overall quantum yields exceeding 0.5 redox pairs per photon absorbed can be realized; for tetrakis(diphosphito)diplatinate(II), tris(4,7-bis(4-sulfonatobenzyl)-1,10-phenanthroline)ruthenate(II), and tris(4,4′-dicarboxylato-2,2′-bipyridine)ruthenate(II) yields are markedly less, a consequence of their shorter intrinsic triplet lifetimes and poor cage escape yields. In the absence of vesicles, product formation is negligible because ion pairing of viologens with sensitizers is extensive, giving rise to static quenching of the photoexcited states. The ionic strength dependence of the kinetics of $^3ZnTPPS^{4-}$ ion oxidation by C_nMV^{2+}–DHP particles suggests a diffusion-controlled mechanism with electron transfer occurring over a distance of separation approximating the hard-sphere collision diameter of sensitizer and viologen. Although the quenching rate constants are determined by the frequencies of collision between vesicles and $^3ZnTPPS^{4-}$, an apparent concentration dependence upon C_nMV^{2+} ions arises because the effective dielectric constant at the reaction site varies with the extent of viologen loading. Recombination of the $ZnTPPS^{3-}$ π-cation with viologen radical cations follows mixed first- and second-order kinetics; possible mechanisms are discussed.

Interfacial adsorption and partitioning reactants between solution microphases are techniques that have been used to modify the chemical reactivity of a wide variety of processes, including photochemical redox reactions.[1] The physical state(s) of the adsorbed reactants are often not well-characterized, particularly when both microphases are fluid, rendering quantitative interpretations of their dynamic behavior difficult. For example, the extent of aggregation of minor components in synthetic mixed vesicles has been shown in several systems to depend upon medium composition, dopant levels, and the structural phase of the vesicles.[2] Furthermore, the simultaneous presence of two or more distinct binding sites within a single vesicle has been inferred from the chemical[3-5] and photophysical[6-9] behavior of a variety of adsorbed substances. Thus, despite the apparent simplicity of these microphase assemblies, their physical properties and dynamic behavior suggest considerable structural heterogeneity of bound reactants.

As part of our effort to develop a conceptual understanding[10] of the phenomenon of transmembrane oxidation–reduction across bilayer membranes[3,11-15] we have sought to characterize the nature of binding of alkylviologens (*N*-alkyl-*N*′-methyl-4,4′-bipyridinium, C_nMV^{2+}) to anionic dihexadecylphosphate (DHP) vesicles. In

†Oregon Graduate Center.
‡Solar Energy Research Institute.

(1) Representative reviews: Fendler, J. H. *Annu. Rev. Phys. Chem.* **1984**, *35*, 137-151. Grätzel, M. *Mod. Aspects Electrochem.* **1983**, *15*, 83-165. Thomas, J. K. *ACS Symp. Ser.* **1982**, *198*, 335-346. Kuhn, H. *Pure Appl. Chem.* **1979**, *51*, 341-352.
(2) Kunitake, T.; Ihara, H.; Okahata, Y. *J. Am. Chem. Soc.* **1983**, *105*, 6070-6078. Nakashima, N.; Morimitsu, K.; Kunitake, T. *Bull. Chem. Soc. Jpn.* **1984**, *57*, 3253-3257.
(3) Ford, W. E.; Tollin, G. *Photochem. Photobiol.* **1983**, *38*, 441-449.
(4) Mizutani, T.; Whitten, D. G. *J. Am. Chem. Soc.* **1985**, *107*, 3621-3625.
(5) Ishiwara, T.; Fendler, J. *J. Am. Chem. Soc.* **1984**, *106*, 1908-1912.
(6) Suddaby, B. R.; Brown, P. E.; Russell, J. C.; Whitten, D. G. *J. Am. Chem. Soc.* **1985**, *107*, 5609-5617.
(7) Schanze, K. S.; Shin, D. M.; Whitten, D. G. *J. Am. Chem. Soc.* **1985**, *107*, 507-509.
(8) Almgren, M. *J. Phys. Chem.* **1981**, *85*, 3599-3603.
(9) Cellarius, R. A.; Mauzerall, D. *Biochim. Biophys. Acta* **1966**, *112*, 235-255.
(10) Hurst, J. K.; Thompson, D. H. P. *J. Membrane Sci.* **1986**, *28*, 3-29.
(11) Mettee, H. D.; Ford, W. E.; Sakai, T.; Calvin, M. *Photochem. Photobiol.* **1984**, *39*, 679-683, and earlier publications cited therein.
(12) Lee, L. Y. C.; Hurst, J. K. *J. Am. Chem. Soc.* **1984**, *106*, 7411-7418.
(13) Runquist, J. A.; Loach, P. A. *Biochim. Biophys. Acta* **1981**, *637*, 231-244.

0002-7863/87/1509-0507$01.50/0

this report, we present results of studies designed to probe reactive sites in C_nMV^{2+}–DHP particles by examining the kinetics of oxidative quenching of photoexcited anions, primarily the triplet [5,10,15,20-tetrakis-(4-sulfonatophenyl)porphinato]zinc(II) ($ZnTPPS^{4-}$) ion. These reactions present striking examples of the use of microheterogeneous systems to modify solution dynamics. In the absence of DHP, negligible photoredox chemistry occurs because under the experimental conditions the metalloporphyrin, for example, is nearly completely ion-paired with viologen, giving rise to static quenching in the photoexcited complex.[16-19] However, C_nMV^{2+} ions bind preferentially to DHP vesicles, whose negative surface charge provides electrostatic repulsive forces sufficient to prevent $ZnTPPS^{4-}$ association.[20] Consequently, formation of discrete photoredox product ions, $ZnTPPS^{3-}$ and C_nMV^{+}–DHP, becomes possible. In these systems cage escape yields are unusually high, approaching in some instances near unit efficiency. Because C_nMV^{+} remains bound to DHP, from which $ZnTPPS^{3-}$ is also repelled, recombination is effectively retarded, with lifetimes of the product ions exceeding 10 ms. These features are highly desirable from the standpoint of solar photoconversion, offering the prospect that similar organizates may find application in practical devices.

Experimental Section

Reagents. *N*-alkyl-*N'*-methyl-4,4'-bipyridinium ions were synthesized by adding the appropriate alkyl bromide to *N*-methyl-4,4'-bipyridinium hydrochloride.[21,22] After exchanging chloride for the bromide counterion, the products were recrystallized from *n*-butyl alcohol until chromatography on silica gel (methanol/H_2O/ethylammonium chloride, 12:12:1)[23] gave single spots. Tetrakis(diphosphito)diplatinate(II) was synthesized following procedures described in the literature;[24,25] the potassium salt was twice recrystallized by fractional precipitation with methanol. Electronic absorption spectra in H_2O agreed with published spectra; solution concentrations were determined[24] by using $\epsilon_{368} = 3.4_5 \times 10^4\ M^{-1}\ cm^{-1}$. Since this complex ion degrades slowly in aqueous media, reagent solutions were always freshly prepared before use. Tetrasodium tris(4,7-bis(4-sulfonatobenzyl)-1,10-phenanthroline)ruthenate(II) ($Na_4Ru(BPS)_3$) and tetrasodium tris(4,4-dicarboxylato-2,2'-bipyridine)ruthenate(II) ($Na_4Ru(BPC)_3$) were donated by Michael Grätzel. Stock solutions were prepared by dissolving weighed quantities of the salts in H_2O. Other chemicals used were best available grade from commercial suppliers; water was purified by using a Corning Megapure deionization–distillation system.

Vesicles were prepared by ultrasonic dispersal of DHP mixtures in aqueous buffers using the flat tip probe of a Heat Systems-Ultrasonics W375 instrument operated at a power setting of 4.0–4.5. Two pulses of 10 min each were applied. The clarified suspensions were then filtered successively through 0.8, 0.45, and 0.22 μm pore size Millipore membrane filters. Alkylviologens were then added by mixing appropriately diluted solutions with vesicles by using a tangential 12-jet flow mixer. This procedure minimizes vesicle aggregation and fusion which occur when concentrated viologen solutions are added in bolus. The C_nMV^{2+}–DHP vesicles were then centrifuged at 100 000 g, 4 °C, for 1 h in a Beckman Model L5-65 Ultracentrifuge, and the pale translucent supernatant fraction was taken for subsequent studies. By following these procedures explicitly, one obtains spherical particles with average radii of about 160 Å and a unimodal, moderately narrow distribution of sizes (polydispersity index $\simeq 0.36$).[26] The number of vesicles per unit volume was calculated from the mean radius, assuming a headgroup surface area[27] of 41 $Å^2$, i.e., 1.5×10^4 DHP molecules per vesicle. The relative amount of DHP forming vesicles was taken to be proportional to the fraction of added viologen that was present after preparative manipulations. This procedure assumes that the viologen distributes uniformly over all forms of DHP in the mixtures. By this criterion, yields for vesicles containing short chain viologens ($n \leq 10$) and for longer chain viologens ($n > 12$) at light to moderate loadings ($DHP/C_nMV^{2+} > 10$) were greater than 90%. At the highest accessible loadings for the long chain analogs, yields were ~70%. Viologen concentrations in the suspensions were determined spectrophotometrically by using previously determined molar extinction coefficients for the alkylviologens on DHP;[28] the spectra, taken on a Hewlett-Packard 8450A instrument, were referenced against DHP vesicles to correct for background scattering.

Kinetic Studies. Aliquots of chromophoric sensitizer were mixed with C_nMV^{2+}–DHP suspensions in a fluorescence cuvette fitted with a rubber septum, and oxygen was purged by bubbling with argon for at least 20 min. The sensitizer was excited by using either the second or third harmonic emission from a Nd:YAG laser (fwhm 15 ns), and the temporal response at the wavelength of interest was recorded on Tektronix 7912 transient digitizers. Changes in transmission of the continuous monitoring light (450 W Xe arc output passed through two Spex monochromators) were detected with a Hamamatsu R955 photomultiplier with its dynode chain truncated at the fifth stage. The signal was amplified ~80 times by a Pacific Instruments wide-band (240 MHz) amplifier and interfaced to an online computer for data storage and analysis. The complete system used for studies with photoexcited $ZnTPPS^{4-}$ ion will be described elsewhere.[29]

Rates of formation of alkylviologen radical cations (C_nMV^{+}) were monitored at 605.6 nm, a wavelength for which absorption by ground and triplet-excited state $ZnTPPS^{4-}$ ion is isosbestic, and decay of $^3ZnTPPS^{4-}$ was followed at 825 nm, where absorption by C_nMV^{+} is inappreciable. Kinetic traces were accumulated for data analysis from 4 to 256 individual flashes, the number depending upon experimental conditions. Data for $^3ZnTPPS^{4-}$ decay were satisfactorily treated by using a linear-least-squares analysis of a single first-order process after subtracting a minor base line component comprising a few percent of the total absorbance; data for C_nMV^{+} appearance and decay were treated by using a nonlinear program for two first-order steps, either simultaneous or consecutive. First-order decay of C_nMV^{+} was not rigorously established, however. Recombination of charge-separated photoredox product ions was usually too slow to record beyond the first half-life with the fast-transient recorder used. Where substantial radical decay could be measured, the kinetics followed mixed first- and second-order behavior.[30] Because recombination was generally inappreciable on the time scale of viologen radical formation, assumption of first-order kinetics for this step did not introduce serious error into determination of the formation rate constants. Goodness-of-fit[30] was based upon appropriate statistical parameters and confirmed by the appearance of random residuals in a graphical display.

The laser flash apparatus used for the photolysis kinetics experiments with other sensitizers has been described.[31] Decay of phosphorescence emission from photoexcited $Pt_2(POP)_4^{4-}$, $Ru(BPS)_3^{4-}$, and $Ru(BPC)_3^{4-}$ ions was followed at 513, 602, and 620 nm, respectively, and recovery of ground-state absorption from photobleached $Ru(BPS)_3^{4-}$ and $Ru(BPC)_3^{4-}$ ions at 473 and 470 nm, respectively. The data were adequately fitted to single-exponential equations, with linearity generally being maintained beyond 4 reaction half-lives.

Other Measurements. Fluorescence intensities for $ZnTPPS^{4-}$ ion were measured by using a Spex Fluorolog/Scamp spectrofluorometer/data analysis system. Exciation was at 556 nm; intensities were determined by integration of the spectral emission over the range 570–770 nm and corrected to infinite absorbance by using the formula $I_\infty = \int_{570}^{770} I_f d\lambda / (1 - \exp_{10}(-A_{ex}))$, where I_f is the zinc(II) porphyrin emission at a particular wavelength, and A_{ex} is its absorbance at the excitation wavelength. Fluorescence lifetimes were measured by using a PRA Model 3000 nanosecond Fluorometer System. The illumination source for continuous photolysis studies was a 100 W Hg–Xe compact arc lamp mounted in

(14) Lee, L. Y. C.; Hurst, J. K.; Politi, M.; Kurihara, K.; Fendler, J. H. *J. Am. Chem. Soc.* **1983**, *105*, 370–373.
(15) Tabushi, I.; Kugimiya, S. *J. Am. Chem. Soc.* **1985**, *107*, 1859–1863.
(16) Kalyanasundaram, K.; Grätzel, M. *Helv. Chim. Acta* **1980**, *63*, 478–485.
(17) Rougee, M.; Ebbesen, T.; Ghetti, F.; Bensasson, R. V. *J. Phys. Chem.* **1982**, *86*, 4404–4412.
(18) Schmehl, R. H.; Whitten, D. G. *J. Phys. Chem.* **1981**, *85*, 3473–3480.
(19) Richoux, M.-C. *Int. J. Solar Energy* **1982**, *1*, 161–167.
(20) Hurst, J. K.; Lee, L. Y. C.; Grätzel, M. *J. Am. Chem. Soc.* **1983**, *105*, 7048–7056.
(21) Pileni, M.-P.; Braun, A. M.; Grätzel, M. *Photochem. Photobiol.* **1984**, *31*, 423–427.
(22) Krieg, M.; Pileni, M.-P.; Braun, A. M.; Grätzel, M. *J. Colloid Interface Sci.* **1981**, *83*, 209–213.
(23) Geuder, W.; Hünig, S.; Suchy, A. *Angew. Chem., Int. Ed. Engl.* **1983**, *22*, 489–490.
(24) Che, C.-M.; Butler, L. G.; Gray, H. B. *J. Am. Chem. Soc.* **1981**, *103*, 7796–7798.
(25) Peterson, J. R.; Kalyanasundaram, K. *J. Phys. Chem.* **1985**, *89*, 2486–2492.
(26) Humphry-Baker, R.; Hurst, J. K.; Thompson, D. H. P., manuscript submitted for publication.
(27) Hunt, E. C. *J. Colloid Interface Sci.* **1969**, *29*, 105–115.
(28) Thompson, D. H. P.; Barrette, W. C., Jr.; Hurst, J. K. *J. Am. Chem. Soc.*, in press.
(29) Connolly, J. S.; Marsh, K. L.; Cook, D. R.; Bolton, J. R.; McIntosh, A. R.; Weedon, A. C.; Ho, T.-F., manuscript in preparation.
(30) Gorman, D. S.; Connolly, J. S. *Int. J. Chem. Kinet.* **1973**, *5*, 977–989.
(31) McNeil, R.; Richards, J. T.; Thomas, J. K. *J. Phys. Chem.* **1970**, *74*, 2290–2294.

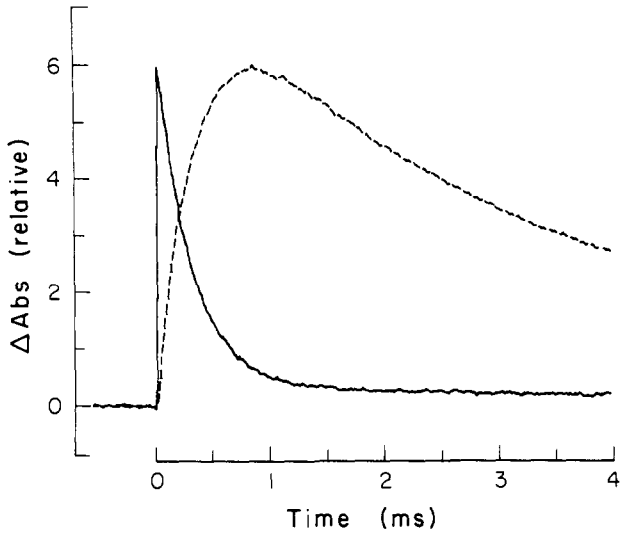

Figure 1. Transient absorption profiles of $ZnTPPS^{4-}$, $C_{16}MV^{2+}$–DHP solutions. Solid line: $^3ZnTPPS^{4-}$ only, 825 nm. Dashed line: $C_{16}MV^{+}$ only, 605.6 nm. Conditions: 20 μM $ZnTPPS^{4-}$, 60 μM $C_{16}MV^{2+}$, 2 mM DHP in 20 mM Tris(Cl), pH 8.0, 23 °C.

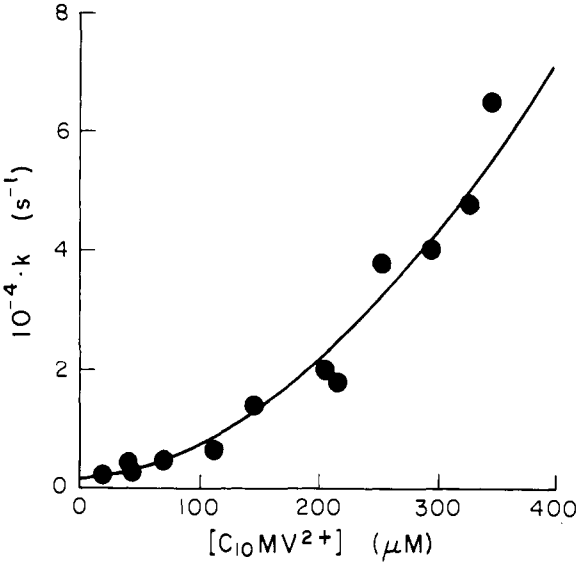

Figure 2. Dependence of $^3ZnTPPS^{4-}$ lifetime upon apparent solution concentrations of $C_{10}MV^{2+}$ ion. Data accumulated from three separate vesicle preparations. Conditions: 6.5 μM $ZnTPPS^{4-}$, 3.6 mM DHP in 20 mM Tris(Cl), pH 8.0, 23 °C. Solid curve, k values calculated according to eq 1 by using the kinetic constants listed in Table I.

an Oriel housing; ultraviolet and infrared emission were removed with 400 nm high-pass and 10 cm pathlength water filters, respectively. Samples were placed in 1 cm optical cuvettes and deoxygenated prior to illumination. Under these conditions, incident light intensities were 1–10 × 10^{-8} einstein/s.

Results

Oxidative Quenching of $^3ZnTPPS^{4-}$ Ion by C_nMV^{2+}–DHP. Triplet state lifetimes of photoexcited $ZnTPPS^{4-}$ are shortened in the presence of C_nMV^{2+}–DHP particles. Loss of absorbance at 825 nm is accompanied by the appearance of absorbing species at 605.6 nm on the same time scale, which then undergoes slow return to the base line absorbance (Figure 1). No perceptible change occurs in the fluorescence lifetime of singlet-excited $ZnTPPS^{4-}$ ion upon addition of C_nMV^{2+}–DHP. These results, taken in conjunction with our previous observations that DHP-bound C_nMV^{+} ions accumulate under continuous photolysis in the presence of sacrifical donors,[20] indicate that $^3ZnTPPS^{4-}$ ion is being oxidatively quenched by the viologens.

Quantitative study of the reactions reveals that their rates are highly dependent upon the identity of C_nMV^{2+}, the number density

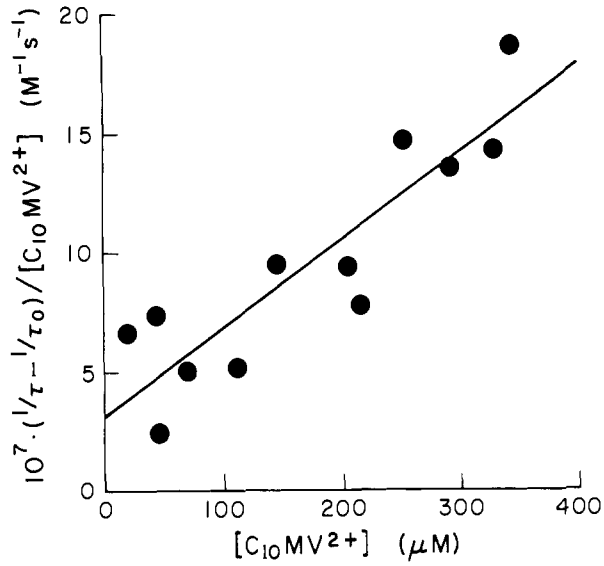

Figure 3. $C_{10}MV^{2+}$–DHP vesicle quenching of $^3ZnTPPS^{4-}$ plotted according to eq 1. Conditions as given in Figure 2. Intercepts (a) and slopes (b) are plotted for each alkylviologen in Figure 4.

Table I. Kinetic Constants for C_nMV^{2+}–DHP Vesicle Quenching of Photosensitizer Ions[a]

n	$10^{-7}a$ (M^{-1} s^{-1})[b]	$10^{-11}b$ (M^{-2} s^{-1})[b]	R[c]
	A. $^3ZnTPPS^{4-}$ ion[d]		
1	109	58.5	0.982
6	4.3	24	0.944
8	10	7.0	0.911
10	3.2	3.6	0.884
12	2.8	0.83	0.981
14	4.7	4.9	0.921
16	2.3	4.5	0.985
16	3.6[e]	1.4[e]	0.996
18		0.68	0.986
20		0.40	0.904
	B. $^3Pt_2(POP)_4^{4-}$		
6	5.0[f]	200[f]	0.961
14	17[f]	17[f]	0.963
16	0.24[g]	6.0[g]	0.978
	C. $^3Ru(BPS)_3^{4-}$[h]		
6		45	0.988
16	19		−0.214
	D. $^3Ru(BPC)_3^{4-}$[i]		
16	150		−0.220

[a] Conditions: 4 mM DHP, 20 mM Tris(Cl), pH 8.0, 23 °C, unless otherwise specified. [b] Defined by eq 1. [c] Correlation coefficient of linear-least-squares data fit. [d] 6.5 μM $ZnTPPS^{4-}$, 3.6 mM DHP, detection at 825 nm. [e] 20 mM (Na)glycine, pH 10. [f] 30 μM $Pt_2(POP)_4^{4-}$, 20 mM $(Na)PO_4$, pH 7.0. [g] 100 μM $Pt_2(POP)_4^{4-}$. [h] 29 μM $Ru(BPS)_3^{4-}$. [i] 50 μM $Ru(BPC)_3^{4-}$.

of vesicles, the C_nMV^{2+}/DHP ratio, and the ionic strength of the medium. Pseudo-first-order rate constants for triplet quenching exhibited marked positive deviations from Stern–Volmer behavior (Figure 2) when plotted against apparent solution concentrations of C_nMV^{2+} ions, but the data could be linearized by adding a second-order concentration term (Figure 3), i.e., by assuming a rate law of the form

$$1/\tau = 1/\tau_0 + a[C_nMV^{2+}] + b[C_nMV^{2+}]^2 \qquad (1)$$

where $1/\tau_0$ is the triplet-state lifetime in the absence of C_nMV^{2+}-DHP vesicles and $[C_nMV^{2+}]$ is the analytical concentration of added viologen. The higher order term was not recognized in earlier work[20] in which the range of C_nMV^{2+} concentration examined was considerably lower.

Experimental values for the kinetic constants determined for various viologens are listed in Table I. As illustrated in Figure 4, quenching rate constants decrease with increasing alkyl chain length on the viologen until n = 6–8, then become relatively

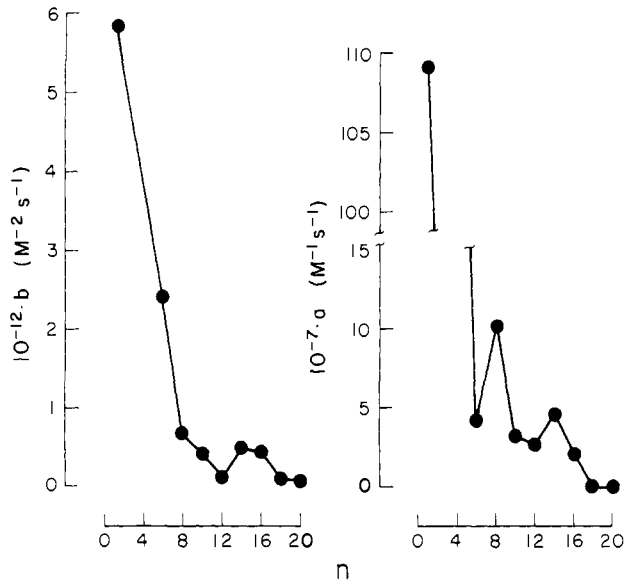

Figure 4. Dependence of kinetic parameters for C_nMV^{2+}–DHP quenching of $^3ZnTPPS^{4-}$ upon alkyl chain length (n). Conditions: 6.5 μM $ZnTPPS^{4-}$, 3.6 mM DHP in 20 mM Tris(Cl), pH 8.0, 25 °C.

Table II. Electrostatic Parameters Controlling $^3ZnTPPS^{4-}$ Reduction of C_nMV^{2+}–DHP Vesicles[a]

n	$[C_nMV^{2+}]$ (μM)	DHP/C_nMV^{2+}	z_Az_B	$10^{-7}k_Q^0$ (M^{-1} s^{-1})[b]	$-z_B$[c]	ϵr[d]
1	171	12	29	74	9.6	189
6	160	12.5	33	8.8	11	160
8	155	13	38	3.7	13	132
10	147	14	31	1.1	10	120
12	116	17	33	1.2	11	129
14	146	14	27	4.0	8.9	117
16	86	23	25	0.63	8.3	93
16	144	14	31	0.83	10	117
16	174	11.5	31	1.3	10	119
16	214	9.3	31	2.0	10	128

[a] In 5–50 mM Tris(Cl), pH 8.0, at 23 °C, $[ZnTPPS^{4-}]$ = 20 μM, [DHP] = 2.0 mM. [b] Defined as $(1/\tau - 1/\tau_0)/[\text{vesicles}]$, where [vesicles] = 0.17 μM under the experimental conditions. [c] Calculated assuming $z_A = -3.0$. [d] Calculated from $k_Q^0 = k_0 \cdot f$ and eq 4, assuming $k_0 = 1.0 \times 10^{11}$ M^{-1} s^{-1}.

independent of the chain length. Rate constants for viologen radical formation are very similar to $^3ZnTPPS^{4-}$ ion decay at low vesicle loadings but are slightly lower at the highest concentration levels examined. Typically the ratio $k(605.6\text{ nm})/k(825\text{ nm})$ = 0.86–1.2 for 0.058–0.27 mM C_6MV^{2+}, with DHP/C_6MV^{2+} varying from 13 to 62; 0.86–1.0 for 0.044–0.33 mM $C_{10}MV^{2+}$, DHP/$C_{10}MV^{2+}$ = 11–81; and 0.83–0.98 for 0.046–0.35 mM $C_{16}MV^{2+}$, DHP/$C_{16}MV^{2+}$ = 10–78. In one set of experiments with $C_{16}MV^{2+}$–DHP, oxidative quenching was found to be insensitive to acidity over the range pH 8–10 (Table I).

Quenching rate constants increase with increasing ionic strength (μ) at constant DHP/C_nMV^{2+} ratios. Results for $C_{16}MV^{2+}$–DHP vesicles at several viologen loadings are displayed in Figure 5. The second-order quenching rate constant k_Q, is obtained by dividing $1/\tau - 1/\tau_0$ by the vesicle "concentration", i.e., the number density expressed as a molar quantity of particles; k_Q plotted against $\mu^{1/2}/(1 + \mu^{1/2})$ allows estimation from the Debye–Huckel limiting law of the apparent electrostatic charge on the DHP-bound viologen and several other physical properties of the reaction sites. Results obtained from analogous plots for various C_nMV^{2+}–DHP vesicles are summarized in Table II; the various parameters recorded are discussed below. One difficult point in the calculations is properly accounting for the contribution of vesicles to the ionic strength, since they constitute inhomogeneous domains of high negative charge that is partially shielded by counterions in the diffuse double layer. This contribution can be assessed empirically by comparing rate constants for photophysical deactivation of

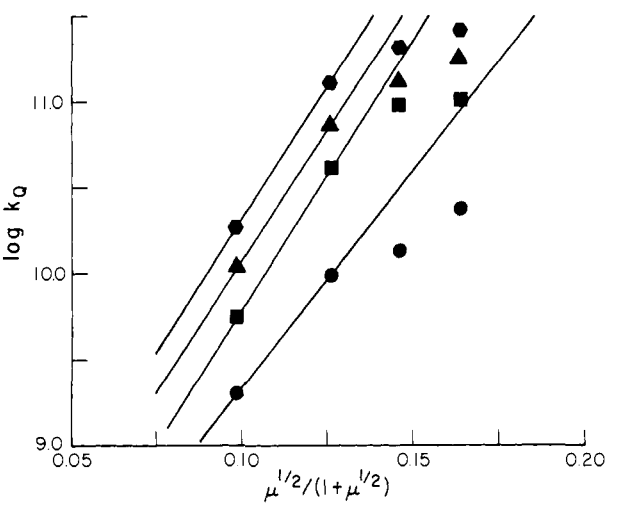

Figure 5. Ionic strength dependence for $C_{16}MV^{2+}$–DHP quenching of $^3ZnTPPS^{4-}$. Conditions: 20 μM $ZnTPPS^{4-}$, 2.0 mM DHP, $[C_{16}MV^{2+}]$, 86 μM (circles), 144 μM (squares), 174 μM (triangles), 214 μM (hexagons). The number density of vesicles, 1.7×10^{-7} vesicles/mL, was calculated from the analytical DHP concentration as described in the Experimental Section. The ionic strength was varied by changing concentrations of the Tris(Cl) buffer; z_Az_B was calculated from the slopes of lines drawn in the figure, which provide estimates of the limiting values at low ionic strength.

$^3ZnTPPS^{4-}$ ion in the presence and absence of vesicles.

Decay of the triplet state of charged metalloporphyrins can show ionic strength dependence when bimolecular quenching mechanisms[32] contribute substantially to overall deactivation. This expectation is realized for the tetracationic [5,10,15,20-tetrakis-(4-methylpyridyl)porphinato]zinc(II) ($ZnTMPyP^{4+}$) ion[33] and, in the present study, for $ZnTPPS^{4-}$ ion. Deactivation under the experimental conditions (920 μM $ZnTPPS^{4-}$, 5–50 mM Tris(Cl), 0–2 mM DHP) exhibits mixed first- and second-order kinetics, i.e.

$$-d[T]/dt = k_1[T] + k_2[T]^2$$

with T = $^3ZnTPPS^{4-}$ ion. Assuming a mechanism comprising three triplet deactivation pathways,[32] i.e.

$$T \xrightarrow{k_T} G$$

$$T + G \xrightarrow{k_{G\text{-}T}} 2G$$

$$T + T \xrightarrow{k_{T\text{-}T}} 2G$$

the constant, $k_1 = k_T + k_{G\text{-}T}[C_0]$, contains terms for all pseudo-first-order quenching (k_T), including impurities,[34] and ground-state bimolecular quenching ($k_{G\text{-}T}$); similarly, $k_2 = k_{T\text{-}T} - k_{G\text{-}T}$ is the difference in bimolecular rate constants for triplet–triplet annihilation and triplet-ground state deactivation. In these equations, G represents the ground state ion and C_0 = T + G. Because $k_{T\text{-}T} \geq 10k_{G\text{-}T}$ for zinc porphyrins,[33,35] $k_2 \simeq k_{T\text{-}T}$. Previous ultrafiltration studies have established that $ZnTPPS^{4-}$ ion does not bind to DHP vesicles.[20] Consequently, increases in the first-order term (k_1) upon adding DHP can be ascribed to increasing ionic strength and/or additional impurity quenching; increases in the second-order term (k_2) are attributable to ionic strength effects on the T–T pathway. The difference in triplet decay rates, plotted as log k_2 against $\mu^{1/2}/(1 + \mu^{1/2})$ with and without 2 mM DHP (not shown) can be quantitatively accounted

(32) Linschitz, H.; Sarkanen, K. *J. Am. Chem. Soc.* **1958**, *80*, 4826–4832. Pekkarinen, L.; Linschitz, H. *J. Am. Chem. Soc.* **1960**, *82*, 2407–2411.
(33) Houlding, V. H.; Kalyanasundaram, K.; Grätzel, M.; Milgrom, L. R. *J. Phys. Chem.* **1983**, *87*, 3175–3179.
(34) McCartin, P. J. *Trans. Faraday Soc.* **1964**, *60*, 1694–1701.
(35) Ballard, S. G.; Mauzerall, D. *J. Chem. Phys.* **1980**, *72*, 933–947. Feitelson, J.; Mauzerall, D. *J. Phys. Chem.* **1982**, *86*, 1623–1628.

Scheme I

$$^3ZnTPPS^{4-} + C_{16}MV^{2+}\text{-DHP} \xrightarrow{1/\tau} ZnTPPS^{3-} + C_{16}MV^{+}\text{-DHP}$$

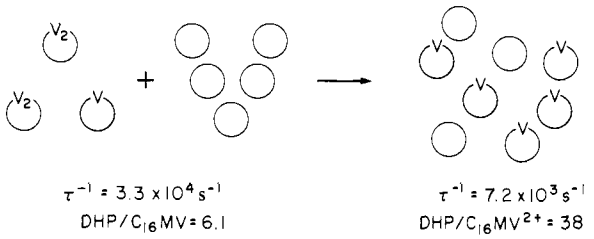

for by assigning a value of μ = 9 mM to the vesicles. Scatter in the data fits precludes accurate determination of the vesicle ionic strength contribution from the k_1 term, although the results are also consistent with this value.

In the two cases examined, with C_6MV^{2+}- and $C_{16}MV^{2+}$-DHP, the quenching rate was found to increase with decreasing number of vesicles at approximately constant concentration levels of added oxidant. For the longer chain analog, preparation of samples with identical $C_{16}MV^{2+}$ ion concentrations is difficult because appreciable viologen-induced aggregation and fusion of vesicles occur during mixing. Nonetheless, the general trend is established qualitatively. The values of $1/\tau$(DHP/C_nMV^{2+}) obtained for 0.25–0.27 mM C_6MV^{2+} are $7.5 \times 10^4\ s^{-1}$ (30), $2.6 \times 10^5\ s^{-1}$ (15), and $9.0 \times 10^5\ s^{-1}$ (4) and for 0.14–0.22 mM $C_{16}MV^{2+}$ are $5.6 \times 10^3\ s^{-1}$ (39), $1.6 \times 10^4\ s^{-1}$ (16), and $4.9 \times 10^4\ s^{-1}$ (6.9).

Because the $^3ZnTPPS^{4-}$ ion lifetime is dependent upon the C_nMV^{2+}/DHP ratio at constant C_nMV^{2+} ion concentrations, it is possible to use measured triplet lifetimes to probe rates of redistribution of viologens among the vesicles. In this experiment, highly loaded and viologen-free vesicles are mixed, and the $^3ZnTPPS^{4-}$ ion lifetime is determined repetitively over succeeding time intervals; decreasing C_nMV^{2+}/DHP ratios arising from dilution onto the viologen-free vesicles will be reflected in increasing triplet lifetimes (Scheme I). Anaerobic suspensions of $C_{16}MV^{2+}$-DHP and viologen-free DHP vesicles were mixed by using syringe-transfer techniques in proportions such that a tenfold decrease in the equilibrium $C_{16}MV^{2+}$/DHP ratio would occur. Specifically, a 0.02 M Tris(Cl) solution, pH 8.0, containing 1.0 mM DHP vesicles and 0.30 mM $C_{16}MV^{2+}$ was mixed with an equal volume of buffer containing 8.0 mM DHP vesicles. Both solutions were 66 μM in $ZnTPPS^{4-}$ ion; the DHP/$C_{16}MV^{2+}$ ratio changed from an initial value of 3.3–30 upon equilibration. Within 2 min, the minimal time required to make the measurements, the lifetime of $^3ZnTPPS^{4-}$, $1/\tau = 6.4 \times 10^3\ s^{-1}$, was found to be essentially the same as the value expected for the fully equilibrated suspensions from measurements made on reference standards (Scheme I) and was unchanged from values measured at subsequent time intervals up to 2 h after mixing. These observations indicate that exchange of viologens between vesicles is rapid ($t_{1/2} \leq 30$ s) with respect to the time required to prepare the samples for kinetic analysis.

The $ZnTPPS^{4-}$, C_nMV^{2+}-DHP photoredox systems exhibit no evidence of physical decomposition. Even after several thousand laser flashes of ~100 mJ at 532 nm, solution spectra were indistinguishable from those of unirradiated samples. The amount of $^3ZnTPPS^{4-}$ formed by the laser flash, measured by initial amplitudes of the kinetic traces at 825 nm, decreased progressively with addition of increasing amounts of C_nMV^{2+}, however. For the longer chain analogues ($n \geq 14$) this effect was relatively small, the amplitudinal loss being less than 25% of the signal intensity in the absence of added C_nMV^{2+}-DHP vesicles, but became increasingly pronounced with shortening of the violgen alkyl chain. In the extreme, methyl viologen at 0.60 mM and MV^{2+}/DHP = 0.17, the highest concentration ratio used, quenched $^3ZnTPPS^{4-}$ absorption in the laser flash experiment by about 67%. In general, addition of C_nMV^{2+}-DHP vesicles did not perturb the $ZnTPPS^{4-}$ optical absorption spectrum, but, for n = 1, 6, 8, extensive loss of triplet absorption intensity in the laser flash studies was accompanied by a distinct bathochromic shift in the zinc porphyrin band maxima, e.g., 554–558 nm for the Q_1 band. Additionally, the fluorescence intensity in C_6MV^{2+}-DHP solutions was diminished maximally by 60% relative to $ZnTPPS^{4-}$ in the absence of viologen, whereas $C_{10}MV^{2+}$- and $C_{16}MV^{2+}$-DHP caused only about 30% and 8% loss of intensity, respectively, at the highest C_nMV^{2+}/DHP ratios investigated. The magnitudes of fluorescence quenching are qualitatively in accord with the loss in initial amplitudes of the corresponding transient kinetic curves.

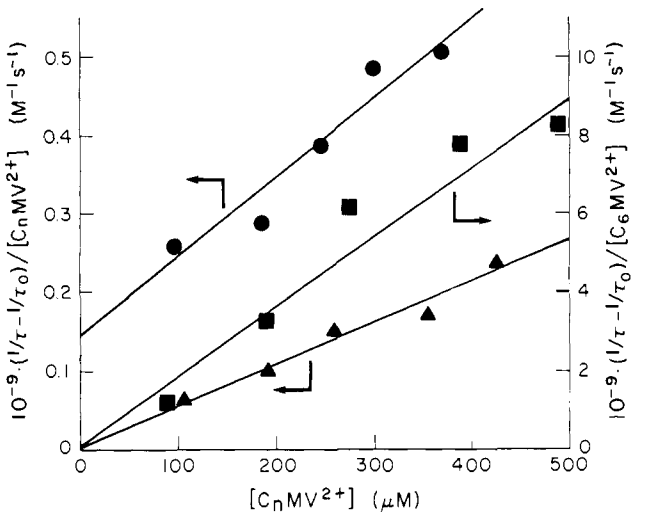

Figure 6. C_nMV^{2+}-DHP vesicle quenching of $^3Pt_2(POP)_4^{4-}$ plotted according to eq 1. Left ordinate, $C_{14}MV^{2+}$ and $C_{16}MV^{2+}$; right ordinate, C_6MV^{2+}. Conditions: for C_6MV^{2+} (squares) and $C_{14}MV^{2+}$ (circles), 30 μM $Pt_2(POP)_4^{4-}$, 20 mM (Na)phosphate, pH 7.0; for $C_{16}MV^{2+}$ (triangles), ~100 μM $Pt_2(POP)_4^{4-}$, 20 mM Tris(Cl), pH 8.0; for all runs, [DHP] = 4 mM, with T ambient (23 °C).

Other Photosensitizers. a. $Pt_2(POP)_4^{4-}$ Ion. Phosphorescence quenching of this sensitizer ion by DHP-bound C_nMV^{2+} ions also exhibited positive deviations from Stern–Volmer kinetics. Three systems were investigated, C_6MV^{2+}- and $C_{14}MV^{2+}$-DHP in 0.2 M phosphate, pH 8.0, and $C_{16}MV^{2+}$-DHP in 0.2 M Tris(Cl), pH 8.0. Data were fitted to the quadratic rate law of eq 1, as shown in Figure 6; the kinetic constants thus derived are included in Table I. The intense luminescence of photoexcited $Pt_2(POP)_4^{4-}$ renders difficult the observation of alkylviologen radical cations, which would confrim an electron-transfer mechanism. For the C_6MV^{2+} and $C_{14}MV^{2+}$ ions, residual absorption is seen after laser excitation in the region of 580–700 nm with maximum intensity at about 610 nm, consistent with some formation of C_nMV^{2+} ions as charge separated products.[10,36] This transient species disappears slowly ($t_{1/2} \simeq 5$ ms) with return of absorbance to its original base line value.

The sensitizer underwent photodecomposition in the laser flash, as was apparent from diminished phosphorescence in samples that had been illuminated. Decomposition was most prominent in Tris-buffered media, where 75–95% of the sensitizer emission was lost after only five flashes. Under comparable conditions, emission intensities decreased less than 20% in H_2O or phosphate buffer. These observations suggest that some form of association of Tris with $Pt_2(POP)_4^{4-}$ may occur, e.g., weak axial ligation by the free amine or ion-pairing with its conjugate acid, that enhances decomposition of the photoexcited ion. Other physical measurements give no evidence of appreciable ground-state association, however. The absorption spectrum is unaltered by addition of buffers or C_nMV^{2+}-bound or unbound DHP vesicles. The first-order luminescent decay constant, $k_0 = 1.1 \times 10^5\ s^{-1}$, was identical in all media and compared favorably with published values obtained in water.[24,25] Measured rate constants for quenching by C_nMV^{2+}-DHP vesicles were also unaffected by the extent of sensitizer photodecomposition.

(36) Meisel, D.; Mulac, W. A.; Matheson, M. S. *J. Phys. Chem.* **1981**, *85*, 179–187.

b. Anionic Ruthenium Complex Ions. Lifetimes for triplet photoexcited $Ru(BPS)_3^{4-}$ and $Ru(BPC)_3^{4-}$ ions in 0.02 M Tris(Cl), pH 8.0, were 3.7 and 0.72 μs, respectively. Rate constants for recovery of ground-state absorption and phosphorescence decay were identical within experimental uncertainty. Addition of DHP vesicles had no effect upon the deactivation rates; lifetimes were shortened by addition of C_nMV^{2+}–DHP. Quenching was far less efficient than for the other sensitizers studied. Thus, for $C_nMV^{2+}/DHP \simeq 0.1$, the highest ratio investigated, quenching of $Ru(BPS)_3^{4-}$ by C_6MV^{2+}–DHP was ~75%, and quenching of either photoexcited ion by $C_{16}MV^{2+}$–DHP was less than 15%. Within a large experimental uncertainty arising from the small amount of quenching, the reactions with $C_{16}MV^{2+}$–DHP vesicles follow the Stern–Volmer rate law. Positive deviations were apparent for C_6MV^{2+}–DHP which, however, was not fitted well by eq 1. Summary data are included in Table I.

As with $Pt_2(POP)_4^{4-}$, viologen radical formation could not be unambiguously assigned from transient spectra in the laser flash studies. However, redox quenching could be demonstrated by continuous photolysis in the presence of appropriate sacrifical donors. Viologen radical formed immediately upon illumination of $C_{16}MV^{2+}$–DHP solutions containing EDTA and $Ru(BPS)_3^{4-}$ ion or 1,4-D,L-dithiothreitol and $Ru(BPC)_3^{4-}$ ion. The latter reaction did not occur if TEOA or EDTA was used as donor. Consistent with previous observations,[20] the viologen radical absorption spectrum in solutions containing DHP vesicles indicated predominantly monomeric species whereas, if vesicles were absent, illumination gave the spectrum of aggregated viologen radical.[36] Sensitizer absorption spectra were unchanged after illumination in either the laser flash or continuous photolysis experiments, indicating negligible decomposition had occurred.

Discussion

Viologen-Vesicle Association. Strong adsorption of C_nMV^{2+} ions to DHP vesicles has been demonstrated by chromatography on dextran gels and strong acid cation exchange resins, by ultrafiltration analyses and by optical absorption spectroscopy.[20] Binding is most obvious from the spectroscopic observation that for the compounds with long chain alkyl substituents ($n \geq 6$), aggregation of the reduced viologen radical cation does not occur in solutions containing the vesicles. Nonetheless, at the higher concentrations used, the physical properties of solutions containing C_nMV^{2+}–DHP and $ZnTPPS^{4-}$ ion indicate that the sensitizer is also partially ion-paired by viologen. Thus, flash-induced yields of $^3ZnTPPS^{4-}$ decrease at higher viologen concentrations in parallel with loss of fluorescence intensity and bathochromic shifting of the sensitizer's visible absorption bands. From the observation that these effects diminish with increasing alkyl chain length, we infer that partitioning onto the vesicles is favored by increased hydrophobic interactions between the alkyl chain and vesicle interior. This interpretation is consistent with chromatographic behavior; methyl viologen can easily be removed from the external surface of DHP by passage through sulfonic acid derivatized polystyrene resins,[14] but the C_6MV^{2+} ion is only partially removed and the longer chain viologens not at all by these procedures.

Mechanisms of Oxidative Quenching of Photoexcited Sensitizer Ions. Reaction of a particle-bound compound with a second reagent in homogeneous solution has generally been treated in terms of a mechanism comprising two pathways, one being the direct bimolecular interaction between reactants at the interface, the other initial adsorption of the solution-phase component followed by surface diffusion of the bound reactants to an appropriate reaction distance. Under certain conditions the indirect pathway can dominate, leading to substantially enhanced second-order rate constants over that expected from simple bimolecular collision.[37] The indirect pathway does not seem to contribute appreciably to the overall reaction in the present instance, however. Its relative contributions are expected to dominate at low interfacial concentrations of the bound reactant, but observed rate enhancements beyond simple Stern–Volmer quenching increase progressively with vesicle loading (Figure 2). At the highest C_nMV^{2+} ion concentrations used, about one-sixth of the ions forming the outer vesicle surface are viologens, conditions which would preclude significant contribution of the indirect pathway if the viologen were randomly distributed on the vesicle surface. Additionally, the strong electrostatic repulsion between the tetraanionic sensitizer ion and negatively charged vesicle should prevent surface association; correspondingly, the physical and photophysical properties of the ions, except ionic strength effects, are unaltered in the presence of DHP.

Assuming bimolecular reaction between sensitizer ions and C_nMV^{2+}-bound DHP vesicles, the rate law for oxidative quenching is given by

$$-d[^3S]/dt = k_Q[^3S][\text{vesicles}]$$

where S is the sensitizer ion, and the apparent vesicle concentration is the number density of particles expressed as a molar quantity, which is calculated from the added concentration of DHP monomer and the average vesicle dimensions. Since bound viologen is in large excess over sensitizer and the vesicle number density is constant, triplet sensitizer decay is expected to be pseudo first order, as was observed (Figure 1). For $ZnTPPS^{4-}$ ion, the quenching rate constant increases with increasing solution buffer concentration, indicating a repulsive interaction between reactant ions (Figure 5). If C_nMV^{2+} ions were to form extensively aggregated cationic "patches" on the vesicle surface, the interaction potential would be attractive. Thus, the salt dependence argues against this sort of lateral phase separation existing in the C_nMV^{2+}-doped vesicles. The quantitative dependence upon salt concentration, valid in the limit of low ionicity, is given by

$$\log k_Q = \log k_Q^0 + 2z_Az_BA\mu^{1/2}/(1 + aB\mu^{1/2}) \qquad (2)$$

where k_Q^0 is the rate constant in pure solvent, z_A and z_B are the electrostatic charges on the reactants, a is the average effective ionic diameter,[38] and A and B are constants that depend on the medium. In water at 23 °C, $A = 0.507$ and $B = 0.328$,[40] so the second term can be approximated as $z_Az_B\mu^{1/2}/(1 + \mu^{1/2})$.

The effective charge on the vesicle (z_B) is unknown but is clearly not the total charge of the particle which, if unshielded, would give, e.g., $-z_B = 10^4$ at $DHP/C_nMV^{2+} \simeq 8$. The effective particle charge can be estimated from the ionic strength dependence according to eq 2. Plots of $\log k_Q$ vs. $\mu^{1/2}/(1 + \mu^{1/2})$ give limiting linear regions whose slopes are z_Az_B (Figure 5). Deviations from linearity at higher salt may be consequences of inherent limitations in the theoretical model, e.g., the assumption of point charges in a dielectric continuum. The effective charge on the $ZnTPPS^{4-}$ ion defined kinetically by its bimolecular deactivation reactions is also less than its total electrostatic charge. From the limiting slope at low ionic strengths, values of $z_A = -2.8$ and -3.2 are calculated for the k_1 and k_2 pathways, respectively. These numbers compare favorably with reported estimates of $z_A = 2.7$ and 1.9 for $ZnTMPyP^{4+}$ ground-state and triplet-state quenching, respectively.[33] Possible reasons for the discrepancies between measured values and simple theoretical expectations for these reactions have been discussed previously.[33,41] Assuming $z_A \simeq -3$ for redox reactions involving $^3ZnTPPS^{4-}$, the effective particle charge at the reaction site can be calculated. Similar techniques

(37) Astumian, R. D.; Chock, P. B. *J. Phys. Chem.* **1985**, *89*, 3477–3482. Adam, G.; Delbrück, M. In *Structural Chemistry and Molecular Biology*; Rick, A., Davidson, N., Eds.; Freeman & Co.: San Francisco, 1968; pp 198–215.

(38) An appropriate value of a for vesicles is unknown. Other researchers have considered using the particle dimensions in examining ionic strength effects in metalloprotein–small molecule redox reactions;[39] this procedure seems inconsistent with treatment of the electrostatic charge, which is assumed to include contributions only from groups in the vicinity of the reaction site. We adopt the procedure of assuming that a is constant for the reactants,[10] a condition which validates eq 2.

(39) Rosenberg, R. C.; Wherland, S.; Holwerda, R. A.; Gray, H. B. *J. Am. Chem. Soc.* **1976**, *98*, 6364–6369.

(40) Manor, G. G.; Bates, R. G.; Hamer, W. J.; Acree, S. F. *J. Am. Chem. Soc.* **1945**, *65*, 1765–1767.

(41) Carapellucci, P. A.; Mauzerall, D. *Ann. N. Y. Acad. Sci.* **1975**, *244*, 214–237.

have been used to determine apparent electrostatic charges at other macromolecular sites, e.g., in redox metalloproteins.[39] In the present instance, the charge remains remarkably constant over the range of alkylviologens investigated (Table II); its value ($z_B \simeq -10$) is very nearly that determined for chemical reduction of $C_{16}MV^{2+}$–DHP by $S_2O_4^{2-}$ ion,[10] for which $z_B \simeq -12$.

Extrapolation to zero ionic strength allows determination of k_Q^0. For an encounter-controlled bimolecular reaction, k_Q^0 is often expressed as $k_Q^0 = k_0 f$, the product of the diffusion-limited rate constant for noninteracting particles (k_0) and an appropriate function (f) of their interaction potential. For spherical symmetry, assuming a Coulomb potential for the charged particles, one obtains from phenomenological theory[42]

$$k_0 = (4\pi N_0/1000) r_{AB}(D_A + D_B) \quad (3)$$

where N_0 is Avogadro's number, r_{AB} is the collision cross section radius, and D_A, D_B are the particle diffusion coefficients and

$$f = \gamma/(e^\gamma - 1), \quad \gamma = z_A z_B e^2/\epsilon r kT \quad (4)$$

where e is the electronic charge, ϵ is the dielectric constant of the medium, and r is the point charge separation distance. Within the context of this treatment, k_0 is independent of the vesicle surface charge, i.e., the extent of C_nMV^{2+} loading. For a given viologen, we had expected that increasing the vesicle loading would, by decreasing the net negative charge on the vesicle, cause a corresponding decrease in z_B. Under these circumstances, if ϵr remained constant, it would be possible to determine a value of ϵr that gave convergence to a common value of k_0, which could then be compared to theoretical interpretations. However, for $C_{16}MV^{2+}$, at least, this relationship does not hold. The effective charge z_B does not vary systematically with DHP/$C_{16}MV^{2+}$ (Table II); consequently the data do not converge when treated in this fashion. An alternative approach is to use the calculated k_0 and measured values of $z_A z_B$ to determine ϵr for each DHP/$C_{16}MV^{2+}$ ratio. By this treatment, ϵr is found to increase as viologen loading on the particle increases (Table II); $k_0 = 1.0 \times 10^{11}$ M^{-1} s^{-1} was used for these calculations, which is the number obtained from eq 3 when the sum of hard-sphere radii $r_{AB} = 165$ Å and D_A-($ZnTPPS^{4-}$) $\simeq 0.8 \times 10^{-5}$ cm^2 s^{-1}. Contribution by the much larger DHP vesicle to the mutual diffusion coefficient was assumed to be negligible.

The distance of closest approach of $ZnTPPS^{4-}$ and DHP sets a minimum point-charge separation distance of $r \simeq 3$–5 Å. Correspondingly, the apparent dielectric constant at the reaction site must be $\epsilon \simeq 20$–40, substantially less than bulk water. These conditions conceivably could be realized if either the bipyridinium were embedded slightly within the hydrocarbon layer at the interface or dielectric saturation of water occurred in the immediate environment of the vesicle surface. The first possibility is consistent with current conceptual views of binding sites for ionophores and lipophilic ions.[10,43] Although phospholipid films contain a strongly bound hydration layer,[44] the dielectric properties of aqueous-membrane interfaces are not well-described. Ordered water is not unambiguously identified by dielectric relaxation measurements,[45] but liposome ζ potentials have been adequately rationalized in terms of models which include a strongly polarized aqueous layer adjacent to the phospholipid head groups.[46] Further, the Stokes shift of fluorescent dansyl groups covalently linked to the amine terminus of phosphatidylethanolamine indicates an effective dielectric constant of $\epsilon = 4$–34 in the aqueous interfacial regions of several neutral and anionic synthetic liposomes;[47] the range reflects a decrease in ϵ of about ten-fold on passing from the liquid crystalline to the gel phase. Similarly, the interfacial ϵ has been estimated at 27–38 for dipalmitoyllecithin vesicles by incorporation of polar merocyanine dyes.[48] These values are typical of dielectric constants determined for water–lipid interfaces in a wide variety of micelles and model membranes[49] and can be contrasted to overall values of $\epsilon = 6$–15 for the vesicle hydrocarbon phase estimated from dielectric relaxation measurements.[45,50] The data therefore appear consistent with a kinetic model involving encounter-limited oxidation of $^3ZnTPPS^{4-}$ by DHP-bound $C_{16}MV^{2+}$ ions with an electron-transfer distance approximating the hard-sphere limit for the particles. The apparent $C_{16}MV^{2+}$ concentration dependence observed at constant vesicle number densities is then actually a dependence upon the DHP/C_nMV^{2+} ratio which derives primarily from variations in ϵr with the extent of vesicle loading. The increase in ϵr that accompanies addition of viologen may simply reflect a decreasing net surface charge, leading to diminished solvent orientation at the interface with attendant ϵ values more nearly approximating bulk water.

Given this interpretation, the form of the analytical rate law for oxidative quenching (eq 1) is fortuitous. As an alternative interpretation, the quadratic term might be assigned to viologen "pairs" that exist as nearest neighbors on the vesicle surface.[10] Then, defining an equilibrium constant, $K_b = [(C_nMV)_2^{4+}]/[C_nMV^{2+}]$, the b term in eq 1 could be identified with $K_b \cdot b' \cdot [(C_nMV)_2^{4+}]$, where b' is the quenching rate constant for the "pair". At all but the lowest vesicle loadings used in these studies, the quenching kinetics are dominated by the b term pathway, which can account for the observed insensitivity of measured $z_A z_B$ values to varying DHP/$C_{16}MV^{2+}$ ratios (Figure 5). For this latter mechanism to be valid, however, electron transfer must be preceded by collisional activation of the reactants, which is inconsistent with the magnitude of the measured rate constants.

The electrostatic parameters are very similar for the other long chain analogues ($n \geq 8$) measured at common DHP/C_nMV^{2+} ratios (Table II), which suggests an invariant structural organization of the reaction centers. However, for C_6MV^{2+} and MV^{2+} ions, quenching rate constants increase rapidly with chain shortening (Figure 4). One possible explanation is that vesicle binding is less extensive, leading to substantial $^3ZnTPPS^{4-}$ reaction with free viologen. Attempts to account quantitatively for aqueous-phase quenching using published values[17] for $ZnTPPS^{4-}$–MV^{2+} ion pair association and Stern–Volmer quenching constants were unsuccessful, probably because all relevant constants are highly ionic strength dependent, and because conditions under which available values were measured do not match ours. In any event, we cannot presently exclude the notion that enhanced rates arise from solution phase quenching. By this mechanism, the negative z_B measured for these reactions would arise from the dominant effects of changing ionic strength upon viologen binding equilibria. An alternative explanation is that the enhanced quenching rates are caused by changes in the nature of vesicle–viologen interactions. Consistent with this view, we have found in a detailed study of DHP vesicle dimensions by quasielastic light scattering[26] that the hydrodynamic diameters appear to increase upon loading with $C_{16}MV^{2+}$, e.g., by 20% when DHP/$C_{16}MV^{2+}$ = 14, but are unchanged with addition of C_6MV^{2+}. This behavior suggests that the long chain viologens may intercalate within the vesicle bilayer, whereas the shorter chain analogs only occupy surface binding sites.[28] Studies designed to improve structural characterization of the interfacial binding are currently underway.

(42) Debye, P. *Trans. Electrochem. Soc.* **1942**, *82*, 265–272.
(43) Anderson, O. S.; Fuchs, M. *Biophys. J.* **1975**, *15*, 795–830. Ketterer, B.; Neumke, B.; Laüger, P. *J. Membrane Biol.* **1971**, *5*, 225–245.
(44) Hauser, H.; Phillips, M. C. *Prog. Surf. Membr. Sci.* **1979**, *13*, 297–413.
(45) Kaatze, U.; Dittrich, A.; Göpel, K.-D.; Pottel, R. *Chem. Phys. Lipids* **1984**, *35*, 279–290, and references therein.
(46) Luzar, A.; Svetina, S.; Zeks, B. *Biochem. Bioeng.* **1984**, *13*, 473–484.
(47) Kimura, Y.; Ikegami, A. *J. Membrane Biol.* **1985**, *85*, 225–231.
(48) Dion, F.; Bolduc, F.; Gruda, I. *J. Colloid Interface Sci.* **1985**, *106*, 465–469.
(49) Lessard, J. G.; Fragata, M. *J. Phys. Chem.* **1986**, *90*, 811–817, and references cited therein.
(50) Redwood, W. R.; Takashima, S.; Schwan, H. P.; Thompson, T. E. *Biochim. Biophys. Acta* **1972**, *255*, 557–566.

Table III. Cage Escape Yields for DHP-Bound C_nMV^+-Radical Cations

n	$[C_nMV^{2+}]$ (μM)	$[C_nMV^+]$ (μM)[a]	$[^3ZnTPPS^{4-}]$ (μM)	% quenched[a]	Φ_{cs}
			Varying Ionic Strength[b]		
1	171	4.2-4.4	6.7-10.3	99-100	0.43-0.63
6	160	1.7-2.8	3.8-5.9	97-100	0.35-0.60
8	155	1.5-1.7	3.5-6.4	79-99	0.33-0.43
10	147	2.0-2.8	5.6-7.2	71-93	0.42-0.55
12	116	2.3-2.7	6.3-7.0	80-96	0.41-0.45
14	146	2.3-2.6	7.0-8.0	71-93	0.40
16	144	1.9-2.9	7.3-8.5	52-86	0.39-0.43
			Varying C_nMV^{2+}/DHP[c]		
6	58-267	0.33-0.64	0.33-1.0	86-99	0.55-0.73
10	44-332	0.28-0.59	0.32-1.1	53-98	0.66-1.0
16	46-350	0.33-0.64	0.98-1.1	44-96	0.61-0.76
16	86-214[b]	0.76-2.7	6.2-7.3	28-94	0.36-0.54

[a] $(1/\tau - 1/\tau_0)/1/\tau$, measured at 825 nm. [b] $[ZnTPPS^{4-}]$ = 20 μM, [DHP] = 2.0 mM, in [Tris(Cl)] = 5-50 mM, pH 8.0, 23 °C. [c] $[ZnTPPS^{4-}]$ = 6.6 μM, [DHP] = 3.6 mM, in [Tris(Cl)] = 20 mM, pH 8.0, 23 °C, except where noted.

Yields of Charge-Separated Product Ions. A minimal reaction sequence adequate to account for the experimental data is

$$ZnTPPS^{4-} \xrightarrow{h\nu} {}^1ZnTPPS^{4-} \quad (5)$$

$${}^1ZnTPPS^{4-} \xrightarrow{k_{ic}} ZnTPPS^{4-} \quad (6)$$

$$ZnTPPS^{4-} + C_nMV^{2+} \overset{K}{\rightleftharpoons} (ZnTPPS^{4-}, C_nMV^{2+})(IP) \quad (7)$$

$$(IP) \xrightarrow{h\nu} *(ZnTPPS^{4-}, C_nMV^{2+})*(IP) \quad (8)$$

$$*(IP) \xrightarrow{k'_{ic}} (IP) \quad (9)$$

$${}^1ZnTPPS^{4-} \xrightarrow{k_{isc}} {}^3ZnTPPS^{4-} \quad (10)$$

$${}^3ZnTPPS^{4-} \xrightarrow{k_T} ZnTPPS^{4-} \quad (11)$$

$$C_nMV^{2+} + DHP \overset{K'}{\rightleftharpoons} C_nMV^{2+}\text{-}DHP \quad (12)$$

$${}^3ZnTPPS^{4-} + C_nMV^{2+}\text{-}DHP \xrightarrow{k_g} ZnTPPS^{4-} + C_nMV^{2+}\text{-}DHP \quad (13)$$

$${}^3ZnTPPS^{4-} + C_nMV^{2+}\text{-}DHP \xrightarrow{k_{et}} ZnTPPS^{3-} + C_nMV^{+}\text{-}DHP \quad (14)$$

Added C_nMV^{2+} partitions between $ZnTPPS^{4-}$ (eq 7) and DHP vesicles (eq 12). The photoexcited sensitizer in the ion pair (eq 8) is statically quenched (eq 9), presumably by electron transfer within the singlet excited state and rapid charge recombination to yield ground-state reactants. Because these reactions occur within the duration of the laser pulse, they do not contribute to lifetime quenching.[51] Singlet excited $ZnTPPS^{4-}$ (eq 5) undergoes physical deactivation (eq 6) or intersystem crossing to the triplet manifold (eq 10), from which it either returns to the ground state (eq 11) or is oxidized within an encounter complex formed with C_nMV^{2+}-DHP particles. Electron transfer from the triplet state of the sensitizer is exergonic ($E°(ZnTPPS^{3-}/{}^3ZnTPPS^{4-}) \simeq -750$ mV,[52] $E°(MV^{2+/+}) = -440$ mV[53] in H_2O); since DHP binding probably stabilizes viologen radical cations, the reaction is irreversible. The encounter complex dissociates either with back-electron transfer to yield ground-state reactants (eq 13) or charge separated ion radicals (eq 14). The rate constants k_{et} and k_g are complex functions of viologen concentrations and DHP/C_nMV^{2+} ratios, e.g., as approximated by eq 1.

The fractional yield of charge-separated products, i.e., cage escape yield, $\Phi_{cs} = k_{et}/(k_g + k_{et})$, can be estimated from amplitudinal changes in the laser flash by using known extinction coefficients for $^3ZnTPPS^{4-}$ and MV^+ ions. The concentration of $^3ZnTPPS^{4-}$ was determined from the initial absorbance change at 825 nm ($\epsilon_{825} = 6 \times 10^3$ M^{-1} cm^{-1})[52] and that of C_nMV^+ from the maximal change at 605.6 nm assuming an extinction coefficient equal to MV^+ ($\epsilon_{606} = 1.3 \times 10^4$ M^{-1} cm^{-1}).[54] Recombination of charge-separated ions is sufficiently rapid to overlap with the radical-forming reaction (Figure 1). Consequently the amplitudinal change at 606 nm underestimates the total yield of C_nMV^+ ion. Since a quantitative rate law describing recombination is not yet available, it is not possible to make an analytical correction for C_nMV^+ ion decay. Approximate corrections were made by extrapolation of exponential growth and initial decay curves to their point of intersection; such corrections increased the maximally measured radical concentrations by 5-10%. Product yields were then calculated from $\Phi_{cs} = [C_nMV^+]/[^3ZnTPPS^{4-}]_Q$, where only the fraction of triplet sensitizer quenched by C_nMV^+-DHP is included in the denominator. Cage escape yields are largely independent of the identity of C_nMV^{2+} ion and exhibit no systematic variation with changing ionic strength or levels of vesicle loading but decrease with increasing sensitizer concentrations (Table III). Optimally, values as great as $\Phi_{cs} = 0.8$ can be achieved. For comparison, in homogeneous solution at reactant concentrations sufficiently low to allow a significant fraction of $ZnTPPS^{4-}$ to exist as the free ion, $\Phi_{cs} \simeq 0.5$ for MV^{2+} quenching.[17] Reported cage escape yields for other sensitizer ions include $Ru(bpy)_3^{2+}$ ($\Phi_{cs} \leq 0.2$),[55] ZnTMPyP^{4+} ($\Phi_{cs} \leq 0.7$, μ-dependent),[19] and for *N,N*-diisopropylviologen sulfonate (PVS) with $Pt_2(POP)_4^{4-}$, $\Phi_{cs} \simeq 1.0$.[25] In these latter cases, ion pairing between reactants is negligible because attractive electrostatic forces are absent. Despite the product ions being oppositely charged, $\Phi_{cs} \simeq 0.8$ for reaction between PVS and ZnTMPyP^{4+}.[55] In general, cage escape yields for DHP-bound alkylviologen appear equivalent to or moderately greater than comparable systems in homogeneous solution.

The overall charge separation quantum yield ($\Phi°$), expressed as viologen radical formed per photon absorbed, is $\Phi° = \rho \cdot \Phi_{isc} \cdot \Phi_Q \cdot \Phi_{cs}$, where ρ is the fraction of sensitizer not statically quenched, $\Phi_{isc} = 0.84$[49] and is the intersystem crossing quantum yield, and Φ_Q is the fraction of $^3ZnTPPS^{4-}$ ion quenched by C_nMV^{2+}-DHP vesicles. By selecting long chain viologen analogues that partition preferentially onto DHP and by using relatively high vesicle loadings to attain favorable quenching rates, it is possible to achieve high overall product yields. For example, in 0.02 M Tris(Cl) solutions containing 0.2 mM $C_{16}MV^{2+}$ and 6.6 μM $ZnTPPS^{4-}$, with DHP/$C_{16}MV^{2+} \simeq 20$, $\rho \simeq 0.9$, $\Phi_Q \simeq 0.9$, $\Phi_{cs} \simeq 0.7$, giving $\Phi° \simeq 0.5$. Therefore, approximately one-half of the absorbed photons are ultimately converted to redox products under these conditions. Comparable values have recently been attained for a system employing ZnTMPyP^{4+} and cationic vesicles prepared from viologen-containing surfactants, but yields were high only when PVS was used as an electron mediator.[56]

The low yield of products in reactions of other photosensitizer ions cannot be attributed entirely to low Φ_Q values. Quenching rate constants are within the same order of magnitude for all sensitizers investigated (Table I); differing Φ_Q values therefore reflect primarily varying triplet lifetimes. Under the experimental conditions, $\Phi_Q = (k_g + k_{et})/(k_T + k_g + k_{et}) \leq 0.6$ for $Pt_2(POP)_4^{4-}$ with $C_{14}MV^{2+}$ and $C_{16}MV^{2+}$ as reductants, but $\Phi_Q \leq 0.98$ with C_6MV^{2+}; for the ruthenium sensitizers, $\Phi_Q < 0.2$ with $C_{16}MV^{2+}$, but $\Phi_Q < 0.7$ for $Ru(BPS)_3^{4-}$ with C_6MV^{2+}. Since ρ and Φ_{isc} for the photosensitizers should be uniformly high, the inability to directly detect C_nMV^+ formation during the laser flash indicates that Φ_{cs} must be low for these sensitizer ions.

(51) Bolleta, F.; Maestri, M.; Moggi, L.; Balzani, V. *J. Phys. Chem.* **1974**, *78*, 1374-1377. Demas, J. N.; Addington, J. W. *J. Am. Chem. Soc.* **1976**, *98*, 5800-5806.
(52) Kalyanasundaram, K.; Neumann-Spallart, M. *J. Phys. Chem.* **1982**, *86*, 5163-5169.
(53) Moser, J.; Grätzel, M. *J. Am. Chem. Soc.* **1983**, *105*, 6547-6555.
(54) Watanabe, T.; Honda, K. *J. Phys. Chem.* **1982**, *86*, 2617-2619.
(55) Prasad, D. R.; Mandal, K.; Hoffman, M. Z. *Coord. Chem. Rev.* **1985**, *64*, 175-190.
(56) Nagamura, T.; Takeyama, N.; Tanaka, K.; Matsuo, T. *J. Phys. Chem.* **1986**, *90*, 2247-2251.

Recombination Kinetics. Mathematical modeling studies of hole–electron recombination in small semiconductor particles[57] indicate that mixed kinetic behavior will obtain when the average number of pairs per particle lies between 0.5 and about 30; recombination is approximated by simple first- or second-order rate laws when the ratios are less or greater, respectively, than this range. From 1–8 μM ^{3}ZnTPPS^{4-} are formed by the laser flash under our experimental conditions, yielding 0.5–4 μM redox product ions or 2–20 pairs per vesicle. Mixed first- and second-order kinetics might therefore arise *if* the ZnTPPS^{3-} π-cation remained associated with the vesicle surface. This latter notion seems untenable in view of the system electrostatics, however. In the absence of π-cation binding, the product pairs become statistically decorrelated, and second-order kinetics will be observed at all ion/vesicle ratios. An alternative mechanism that could introduce first-order character into the recombination kinetics comprises ZnTPPS^{3-} ion pairing with C_nMV^{2+} in an encounter complex at the vesicle interface, followed by electron exchange between the sensitizer associated C_nMV^{2+} and a neighboring C_nMV^{+} ion. In this model, the interfacial electrostatics dictate preferential approach of the trianionic π-cation to dipositive viologen; EPR spectroscopy has provided evidence consistent with rapid electron exchange between vesicle-bound $MV^{2+/+}$ ions.[58] The two kinetic models give different rate laws and can perhaps be distinguished by the study of recombination dynamics currently in progress.

Acknowledgment. J.K.H. and D.H.P.T. express gratitude to Michael Grätzel for use of his laser flash kinetic facilities at EPFL, Lausanne, Switzerland, and to Michael Grätzel and Guido Rothenberger for enlightening discussions regarding interfacial reaction mechanisms. This work also benefited from the expert technical assistance of Ken Marsh and John Hurley at SERI, Golden, Colorado. Financial support was provided by the Division of Chemical Sciences, Office of Basic Energy Sciences, U.S. Department of Energy through contracts to J.K.H. (DE-AC-06-83ER13111) and J.S.C.

(57) Rothenberger, G.; Moser, J.; Grätzel, M.; Serpone, N.; Sharma, D. K. *J. Am. Chem. Soc.* **1985**, *107*, 8054–8059.

(58) Takuma, K.; Sakamoto, T.; Matsuo, T. *Chem. Lett.* **1981**, 815–818.

Evidence for a Reversible Electrophilic Step in Olefin Bromination. The Case of Stilbenes

Giuseppe Bellucci,* Cinzia Chiappe, and Franco Marioni

Contribution from the Istituto di Chimica Organica, Facoltà di Farmacia, Università di Pisa, 56100 Pisa, Italy. *Received June 5, 1986*

Abstract: Bromonium–bromide ion couple intermediates have been generated by reacting *erythro*- and *threo*-2-bromo-1,2-diphenylethanol with gaseous HBr in 1,2-dichloroethane and in chloroform. It has been shown that in both solvents these intermediates mainly collapse to *meso*-1,2-dibromo-1,2-diphenylethane but also release Br_2 to give *trans*-stilbene. The ratios of *trans*-stilbene to the meso dibromide obtained in all these reactions ranged between 9:91 and 22:78. The product distributions of the additions of HBr and of Br_2, both in the absence and in the presence of HBr, have also been determined. *cis*-Stilbene rapidly added HBr in both solvents, but in 1,2-dichloroethane isomerization to *trans*-stilbene also occurred to a large extent. *trans*-Stilbene mainly underwent oligo- or polymerization. The reactions of both olefins with Br_2 were found to be not stereospecific. In the presence of HBr, the bromination of *trans*-stilbene became anti stereospecific, but in the case of *cis*-stilbene it maintained only a very modest stereoselectivity, and in chloroform HBr addition was predominant. The kinetics of bromination of both *trans*- and *cis*-stilbene in 1,2-dichloroethane were shown to follow very cleanly a third-order rate law (second order in Br_2). However, the product analysis during the bromination of *cis*-stilbene showed that significant amounts of the trans olefin were always present at incomplete conversion. It has been shown that the latter olefin is formed by Br_2-catalyzed isomerization of the starting cis olefin. All these results can be rationalized by assuming that the formation of bromonium–bromide or bromonium–tribromide ion pair intermediates in the discussed reactions is actually reversible.

In spite of its intensive investigation,[1] the mechanism of olefin bromination, in appearance one of the simplest standard textbook organic reactions, is still the object of debate. The stepwise nature of the addition has been recognized for a long time, but important features of the reaction steps are continuously being brought to light.[2-5]

At least four alternative nonradical mechanistic pathways, all of which involve olefin·Br_2 charge-transfer complexes (CTCs),

Scheme I

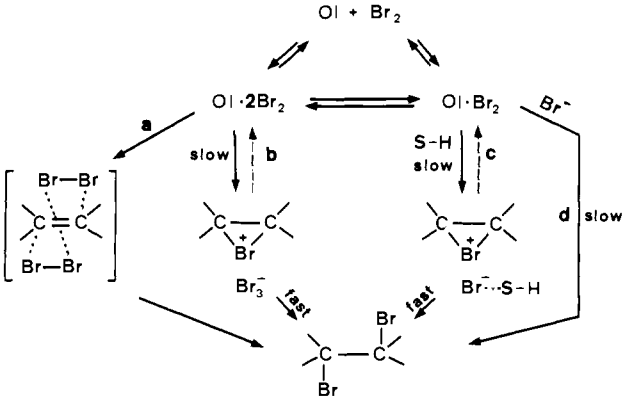

appear to have been proved for the bromination in low polarity nonnucleophilic aprotic solvents, where the reaction is not complicated by the formation of solvent-incorporated products.

The first pathway (a in Scheme I) has been proposed for the slow brominations in apolar solvents like carbon tetrachloride[6]

(1) For extensive recent reviews of olefin brominations, see: (a) Schmid, G. H.; Garratt, D. G. *The Chemistry of Double Bonded Functional Groups*; Patai, S., Ed.; Wiley: New York, 1977; Suppl. A, Part 2, p 725. (b) V'yunov, K. A.; Ginak, A. I. *Russ. Chem. Rev. (Engl. Transl.)* **1981**, *50*, 151–163. (c) De la Mare, P. B. D.; Bolton, R. *Electrophilic Additions to Unsaturated Systems*, 2nd ed.; Elsevier: New York, 1982; pp 136–197.

(2) (a) Ruasse, M.-F.; Zhang, B.-L. *J. Org. Chem.* **1984**, *49*, 3207–3210. (b) Ruasse, M.-F.; Lefebvre, E. *J. Org. Chem.* **1984**, *49*, 3210–3212.

(3) (a) Fukuzumi, S.; Kochi, J. K. *Int. J. Chem. Kinet.* **1983**, *15*, 249–266. (b) Fukuzumi, S.; Kochi, J. K. *J. Am. Chem. Soc.* **1982**, *104*, 7599–7609. (c) Fukuzumi, S.; Kochi, J. K. *J. Am. Chem. Soc.* **1981**, *103*, 2783–2791.

(4) Brown, R. S.; Gedye, R.; Slebocka-Tilk, H.; Buschek, J. M.; Kopecky, K. R. *J. Am. Chem. Soc.* **1984**, *106*, 4515–4521.

(5) Bellucci, G.; Bianchini, R.; Ambrosetti, R. *J. Am. Chem. Soc.* **1985**, *107*, 2464–2471.

0002-7863/87/1509-0515$01.50/0